THE JOURNAL OF PHYSICAL CHEMISTRY B

ARTICLE

pubs.acs.org/JPCB

New Insights into Response Functions of Liquids by Electric Field-Resolved Polarization Emission Time Measurements

Margaret A. Hershberger, Andrew M. Moran,† and Norbert F. Scherer*

Department of Chemistry and the James Frank Institute, The University of Chicago, 929 East 57th Street, Chicago, Illinois 60637, United States

Supporting Information

ABSTRACT: We resolve information about the dynamics of simple liquids that has been obscured in prior frequency and time-domain measurements by way of full field-resolved polarization emission time (FR-PET) measurements of carbon disulfide. The amplitude and phase of the field-resolved transient-grating signal is used to calculate a spectrogram of the signal field at each delay between the transient-grating (TG) pump and probe pulses. The temporal maximum of the spectrogram, defined to be the signal emission time, varies with pump−probe delay; it follows the convolution of the TG pulses while the pulses overlap and exhibits recurrences at times when the nuclear dynamics are the main component of the liquid material response. Since this is a third-order nonlinear spectroscopic method, the isotropic and anisotropic signals are constructed from the polarization tensor components. The frequency-integrated anisotropic component of the signal is equivalent to the signal measured in optical Kerr Effect (OKE) experiments. The FR-PET determination of the signal emission times is a direct measurement of the third-order nonlinear (polarizability) polarization and, hence provides new strong constraints on appropriate models of the liquid dynamics. Models for the material response function are used to calculate the signal emission times. In particular, we show that the proper treatment of the time-correlation function for orientational motion gives the best fit to the FR-PET data for rotational diffusional motion. We also establish that librational motion is not a short-time (coherent) motion that leads to rotational diffusion. Finally, we find that the Bucaro−Litovitz form for interaction-induced dynamics is not entirely correct for the CS_2 liquid we study. We suggest that the failing may result from the implicit assumption of two-body interactions, which is only appropriate for gases.

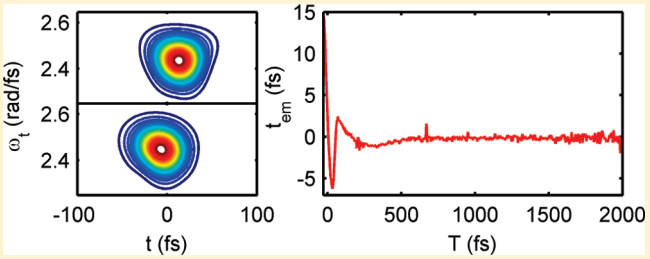

INTRODUCTION

While the course of a chemical reaction is usually understood in terms of the progress from reactants to products, the reactive species in solution are coupled to motions of the solvent molecules. These fluctuations of the solvent molecules provide an energy bath that is coupled (back to) to the reactive species and can hinder or facilitate the reaction. The spectral densities of these solvent fluctuations in response to changing dipoles[1−4] and photoinduced charge transfer reactions have recently been studied.[5−9] However, these low frequency motions do not consist of well-defined modes and the actual molecular motions involved in these spectral densities are incompletely understood.[10] To more completely identify the motions of solvent molecules that influence or are influenced by a reaction, it is necessary to develop a good understanding of, and appropriate analytical models for, the range of fluctuations found in a pure liquid. Previous measurements have not been sufficiently sensitive to the nuclear fluctuations to determine unambiguous analytical forms for the nuclear response functions. As a result, the functional forms that are typically used to describe the intermolecular motions are incorrect in that they contain arbitrary terms or have been defined in an intuitive but ad hoc fashion.

We use full field-resolved polarization emission time (FR-PET) measurements, which are a new extension of field-resolved transient-grating (FR-TG) spectroscopy,[11] to determine the intermolecular motions of CS_2. Specifically, we apply PET measurements to more accurately determine the veracity of commonly used molecular response functions and to demonstrate better functional forms that have a rigorous basis. Electronic and nuclear responses both contribute to the measured signal and modulate the amplitude of the spectral phase of the signal field. These phase modulations are observed as temporal shifts in the maximum of the signal field relative to the TG probe field. Signal emission times for the anisotropic CS_2 response are compared to those calculated using a minimal model of the TG signal field. We find that the instantaneous electronic response dominates at negative and short TG pump−probe delays, where the signal emission time follows the convolution of the pump and probe pulses, while the intermolecular nuclear

Special Issue: Shaul Mukamel Festschrift

Received: December 12, 2010
Revised: March 14, 2011
Published: March 30, 2011

response determines the recurrences seen in the emission time once the temporal overlap between the pump and probe pulses ceases. The signal emission time separates the rise of the intermolecular nuclear responses from the decay of the electronic responses, so fitting the molecular response functions to the signal emission times also necessitates corrections to the functional form of the rotational diffusion term of the nuclear response function.

The relationship between the material response function and the signal emission times is determined through calculations of the FR-PET experiment. The TG signal is proportional to the third-order polarization induced in the sample by the pump and probe pulses.[12]

$$E_s(t,T) = \frac{i2\pi l\omega_\tau}{n(\omega_\tau)c}P^{(3)}(t,T) \quad (1)$$

where ω_τ is the carrier frequency of the signal field, l is the interaction length, the sample refractive index $n(\omega_\tau)$ is constant and

$$P^{(3)}(t,T) = \int_0^\infty dt_3 \int_0^\infty dt_2 \int_0^\infty dt_1\, R^{(3)}(t_3,t_2,t_1)\, E_3(t-t_3) \cdot E_2(T+t-t_3-t_2)\, E_1^*(T+t-t_3-t_2-t_1) \quad (2)$$

Hence, $R^{(3)}$ is the third-order material response function of CS_2, E_3 is the electric field of the probe pulse, E_1 and E_2 are the electric fields of the pump pulses, and each field E_j interacts with the sample at t_j. Since the anisotropic response contains no electronic transitions, we assume that the material dephasing time is instantaneous in t_1 and t_3. With the additional constraint that the probe pulse interacts with the sample after the pump pulses, we can simplify the third-order polarization to

$$P^{(3)}(t,T) = E_{pr}(t)\int_0^\infty dt_2\, R^{(3)}(t_2)\, E_{pu}(T+t-t_2)^2 \quad (3)$$

where E_{pr} is the probe electric field and E_{pu} is the pump pulse electric field. The maximum of $P^{(3)}(t,T)$ for each T is the signal emission time, i.e., the PET signal.

BACKGROUND

Femtosecond time-resolved optical Kerr effect (OKE) spectroscopy has been used to measure the spectral density of intermolecular fluctuations in many pure and mixed fluids.[13−33] The OKE signal exhibits an instantaneous electronic hyperpolarizability response followed by the slower nuclear relaxation. The electronic response can be deconvoluted from the OKE signal,[16,17,24] and the remaining nuclear response is decomposed according to the types of motions involved. Diffusive reorientational motion, responsible for the long-time exponential decay behavior of the OKE signal, is typically given by:[24,31]

$$R_{RD}^{(3)}(t) = a_{RD}e^{-t/\tau_{RD}}(1-e^{-t/\tau_{rise}}) \quad (4)$$

where a_{RD} is the amplitude, τ_{RD} is the rotational diffusion time constant, and τ_{rise} is the time constant that models the rise of the rotational diffusion dynamics. It is useful to subtract the rotational diffusion decay from the OKE signal.[16,17,24,31] The remaining spectral density is generally attributed to librations, hindered rotations, and interaction-induced (II) motions from dipole−induced dipole interactions.[24,31]

The functional forms and assignments of the librations and II motions are still uncertain.[10] Furthermore, these dynamics, and the orientational diffusion, are only captured with limited sensitivity by OKE or transient-grating[14,15] spectroscopy. Analytical models of the nuclear response are underdetermined by either the spectral density or the temporal profile of the response. In general, librational motions occur on the shortest time scales (highest frequency) and II motions on an intermediate time scale (relative to the orientational diffusion).[24,31] This is perhaps most clearly illustrated for the case of water.[21] It is also reasonable to assume that cross-terms between these canonical forms may be significant, as has been shown in molecular dynamics simulations of CS_2[34−37] and benzene.[10] Instantaneous normal-mode analysis of CS_2 and benzene spectral densities show that II scattering contains an orientational component as well as a translational component,[10,31] so these canonical definitions of the motion are more descriptive than accurate. Nevertheless, in the absence of other options, we will use them here.

Librations and II motions are treated separately in phenomenological models. An antisymmetrized Gaussian, a heuristic model, is often used to describe the spectrum of the librational motion:

$$R_L^{(3)}(\omega) = a_L[e^{-(\omega-\omega_0)^2/\Delta\omega^2} - e^{-(\omega+\omega_0)^2/\Delta\omega^2}] \quad (5)$$

where a_L is the amplitude, ω_0 is the central frequency, and $\Delta\omega$ is the width of the distribution of librational modes.[24,30,31] The II motion is usually treated with a modified exponential decay, sometimes of the same form as the rotational diffusion, based on the observation that the intermediate time-scale motions also appear to have an exponential decay.[24,31] The II motion[10,24,31] is also represented in the frequency-domain form introduced by Bucaro and Litovitz[38] to describe collision-induced motions measured in Raleigh scattering spectra of atomic and molecular liquids:

$$R_{II}^{(3)}(\omega) = a_{II}\omega^b e^{-\omega/\omega_{II}} \quad (6)$$

Here, a_{II} is the amplitude, ω_{II} sets the decay of the II response, and b is a dimensionless constant. Although b is treated as a fit parameter, it is related to the distance dependence of the molecular polarizability for a pairwise collision, $\Delta\alpha(r)$, through

$$\Delta\alpha(r) \propto r^{-(7b+14)/2} \quad (7)$$

and has a theoretical value of 12/7, based on the assumption that the polarizability change is proportional to the repulsive interaction between the molecules.[38]

Although the third-order nonlinear responses of simple liquids have been widely studied,[13−33] measurements heretofore have been of the (time and/or frequency) integrated material polarization response. This integration can, of course, obscure aspects of the molecular response, particularly when rapid dynamics occur together with slow features that may be of larger amplitude. The present study is an approach to remove this integration and thereby clearly reveal dynamics that have been obscured and thus incorrectly modeled in prior studies.

FR-TG spectroscopy measures the full field generated by the third-order material polarization and can be compared to other experiments through the selection of specific tensor elements of the signal. Linearly polarized pump pulses select a distribution of CS_2 molecules aligned with the pump field and induce a torque on those not aligned with the field (or cause electrostriction, a density fluctuation). The decay of the transient grating of these molecules is probed by a third polarized field and the full (i.e., real and imaginary) signal field is measured by spectral interferometry. By constructing the anisotropic signal fields from the measured tensor components, the nuclear (and electronic) response measured in FR-TG is identical to that measured in OKE spectroscopy.

Field-resolved measurements offer significant advantages over simple time- or frequency-resolved measurements since the entire electric field of the signal, both amplitude and phase, is determined. Frequency-domain measurements of a signal as a function of the delay between pump and probe pulses are commonly used to determine pulse characteristics (intensity and relative phase) in frequency-resolved optical gating (FROG) measurements.[39] Spectral interferometry, using heterodyne detection (interference of the signal field with a local oscillator field of known delay relative to the pump pulses), allows complete determination of the complex electric field (dispersive and absorptive components).[40−43] Spectral interferometry techniques have been used in pulse characterization[43,44] linear[45,46] and nonlinear[41,42,47−57] spectroscopies. Full field-resolved measurements, both linear[45,46] and nonlinear[11,42] spectrograms, have been shown to reveal novel information compared with conventional (frequency or time integrated) spectroscopies. For example, field-resolved linear measurements allow distinguishing between homogeneous and inhomogeneous lineshapes, and dynamics.[46] The phase sensitivity, as seen in the signal emission times, has been used to distinguish different signal pathways and nonresonant signals from others in third-order and fifth-order nonlinear spectroscopies.[7,11]

EXPERIMENTAL METHODS

Our FR-TG measurements were performed using pulses from a home-built cavity-dumped Ti:sapphire laser, described previously.[58] The pulses were precompensated to a fwhm duration of 30 fs at the sample using a BK7 prism pair. A 25% beam splitter was used to generate a probe pulse with variable delay, T (Newport delay stage, PM400) relative to the pump pulse. Pump and probe pulse pairs were generated and arranged in a BOXcar geometry with a diffractive optic (Holoeye, 10 degrees between ± 1 order). The diffractive optic establishes the (sufficiently) stable phase relationship between the pulses in each pair, which is passively maintained by using common optics for the four pulses. The pulses were focused into the CS_2 sample (Sigma Aldrich, HPLC grade, used without further purification). One pulse from the probe pulse pair was attenuated 10 000-fold with a reflective neutral density filter for use as a local oscillator (LO). Interaction of the sample with the two pump pulses and one probe pulse generated a signal collinear with the LO. Additional glass was inserted to delay the probe pulse so that the LO interacted with the sample at a fixed delay of ~1.3 ps before the probe. (Glass was also inserted into the path of the pump pair to match the dispersion in the probe and LO.) Only signals associated with the TG process were observed; i.e., no changes in the LO intensity or phase were observed due to interaction of the pump pulses with the LO. Matched half-waveplates (Karl Lambrecht) in the probe and local oscillator beams were used to define and measure the *ZZZZ* and *YYZZ* tensor elements of the response. The signal and collinear local oscillator were dispersed in a spectrometer (SPEX M270, 600 grooves/mm grating) and collected with an array detector (Andor iDUS 420DU) as a function of T, the delay between the pump and local oscillator.

The molecular signal at each delay, T, was measured through heterodyne detection, so the total measured frequency dependent intensity, I_{tot}, at the frequency of the laser, ω, is given by

$$I_{tot}(\omega,T) = |E_S(\omega,T)|^2 + |E_{LO}(\omega)|^2 + E_S(\omega,T)\,E_{LO}(\omega,T)e^{\{-i[\psi(\omega) - \omega t_{LO}]\}} \quad (8)$$

where $|E_S(\omega,T)|^2$ is the intensity of the molecular signal field, $|E_{LO}(\omega)|^2$ is the intensity of the LO field, and the third term is the interference between the two fields, which oscillates with a period determined by the delay between the local oscillator and probe pulses, t_{LO}. The phase difference between the signal and local oscillator fields is $\psi(\omega)$. The molecular signal intensity is a small contribution to the total measured intensity. The LO contribution was removed by subtracting the signal intensity measured at approximately $T = -1.5$ ps from the measured intensity at each T. (By causality, the signal at $T = -1.5$ ps does not contain any components associated with the T-dependent transient-grating response.) Any additional contribution of the LO to the signal was removed in the Fourier transform processing.[11,40]

RESULTS

The isotropic and anisotropic signals of the CS_2 TG response are determined by linear combinations of the E_{ZZZZ} and E_{YYZZ} tensor elements.[59,60] The signal associated with each tensor element is measured separately and the response scaled for the experimentally determined polarization-dependent differences in the LO and probe transmission. The anisotropic signal E_{aniso} and isotropic signal E_{iso} are given by

$$E_{aniso}(\omega,T) = \frac{E_{ZZZZ}(\omega,T) - E_{YYZZ}(\omega,T)}{2} \quad (9)$$

$$E_{iso}(\omega,T) = \frac{E_{ZZZZ}(\omega,T) + 2E_{YYZZ}(\omega,T)}{3} \quad (10)$$

Processing of the heterodyne detected signal gives the real and imaginary components (corresponding to the absorptive and dispersive molecular responses), or amplitude and phase, of the transient-grating signal. For a nonresonant process, such as the one studied here, the absorptive component is small. The phase of the signal field (relative to the local oscillator) is determined by subtracting the phase differences between the probe and local oscillator fields from the oscillatory component of the measured signal. These phase differences result from the time delay and slight difference in material propagation distance between the probe and local oscillator fields. The time delay between probe and local oscillator pulses is determined by the period of the oscillatory component of the full signal. Differences in material propagation distance give rise to the constant phase difference, $\psi(\omega)$ from eq 8, which is determined from the residual phase of the isotropic response at zero delay between the pump and probe pulses. At zero delay, the isotropic response is due to the electronic (hyper)polarizability only, which should have a constant spectral phase for well-compressed pulses. (The third-order polarization has spectral phase of zero for this response, resulting in a constant phase of $\pi/2$ for the signal.)

The imaginary components of the frequency-resolved and frequency-integrated isotropic and anisotropic signal fields from CS_2 are shown in Figure 1. Both signal fields are convoluted with the LO field; however, this has minimal effect on the reconstructed field since the spectral envelope of the signal does not change with delay. The anisotropic signal shows a peak at $T = 0$, when the pump and probe pulses overlap in the sample. As T increases, the signal slowly rises to a second peak at nearly 200 fs, followed by an even slower decay. The frequency-integrated anisotropic signal corresponds to the amplitude of the signal measured in an OKE experiment. The isotropic signal contains a large amplitude peak when all pulses overlap in the sample, which is used to determine the pulse duration.

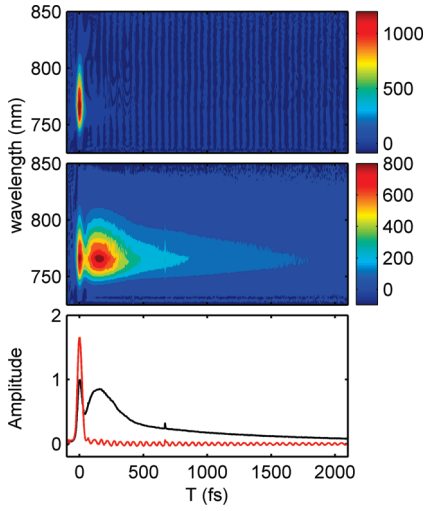

Figure 1. Isotropic (top) and anisotropic (middle) responses of CS2 calculated from the measured *ZZZZ* and *ZZYY* tensor elements. The frequency integrated anisotropic (black) and isotropic (red) responses are shown in the bottom panel.

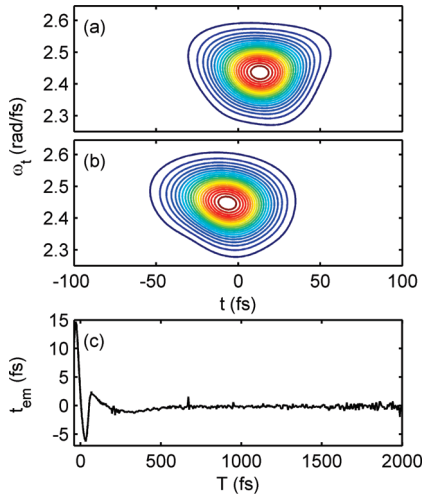

Figure 2. Spectrograms calculated for $T = -30$ fs (a) and $T = 30$ fs (b) showing a shift in the peak amplitude relative to the arrival of the probe pulse (at $t = 0$). (c) This shift in signal emission time, t_{em}, is shown for each delay T.

The long time isotropic response consists mainly of a small amplitude oscillatory component that corresponds to the strongly polarized Raman active totally symmetric stretch of CS_2 at 656.5 cm^{-1}.[61]

Spectrograms of the signal field show the instantaneous frequency of the signal field as a function of time, t, for each delay T. A spectrogram $\Phi(\omega_t t)$ of the signal field can be calculated for each delay T as[39]

$$\Phi(\omega_t,t,T) = \left| \int_{-\infty}^{\infty} E_s(\tau,T)\, g(t-\tau)\, \exp(-i\omega_t \tau)\, d\tau \right|^2 \quad (11)$$

where E_s is the signal field and $g(t)$ is a gate pulse set to have the same duration as the probe pulse. Representative spectrograms are shown in Figures 2a,b for delays of -30 and $+30$ fs. The signal field is always centered at the wavelength of the LO, 770 nm, but the position of the field's temporal maximum shifts in time. The time at which the maximum of the signal field occurs relative to the time the probe pulse arrives in the sample is defined as the signal emission time, t_{em}. Positive signal emission times, as observed at negative T, indicate that the maximum of the emitted field occurs after the maximum of the probe pulse arrives in the sample. Similarly, when $t_{em} < 0$, the signal field maximum occurs before the maximum of the probe pulse. These signal emission times are calculated by finding the center of a Gaussian function that is fit to the temporal profile of the spectrogram (Figure 2c).[7,11] A discussion of the choice of method for calculating the signal emission time can be found in the Supporting Information.[62]

The dependence of the signal emission time on pump−probe delay is not trivial. As shown in Figure 2c, the signal emission time decreases linearly near $T = 0$, then sharply increases at approximately 40 fs, and decreases again until a second recurrence occurs around 300 fs. At long delays, the emission time is nearly constant and slightly negative until the signal amplitude is so small that the emission time cannot be determined. While the precision of determining the signal emission time is very good (standard deviation = 0.1 fs for t_{em} determined from Gaussian fits to the spectrogram at T with relatively large signal amplitudes) its accuracy is limited by the ability to determine the delay between probe and local oscillator pulses. The signal emission times are corrected for errors in the probe to LO delay by calculating the asymptotic value of t_{em} at long T. As described below, the long time behavior of t_{em} depends on the rotational diffusion term. The asymptotic value of t_{em} calculated with a rotational diffusion time constant of 1.7 ps (determined from a fit of the frequency-integrated anisotropic response and literature values[30]) and 30 fs fwhm pulse duration gives a correction of about 2 fs, which is added to t_{em} at all delays.

The signal emission time, or PET, is equivalent to the group delay of the emitted field. It is given by the derivative of the spectral phase of the transient-grating signal[39]

$$t_{em} = \frac{d\varphi(\omega_t,t,T)}{d\omega_t} \quad (12)$$

where φ is the spectral phase of the signal given by

$$\varphi(\omega_t,t,T) = -\arctan\left[\frac{\mathrm{Im}\, E_s(\omega_t,t,T)}{\mathrm{Re}\, E_s(\omega_t,t,T)}\right] \quad (13)$$

Thus, the emission time reflects changes in the spectral phase of the signal. The emission time is most sensitive to variation in the signal field when either the absorptive or dispersive component of the signal is small, as is the case for this off-resonant measurement of CS_2. (Since $\arctan(1/x) = -\arctan(x) \pm (\pi/2)$, if either component of the field is small, the derivative of the spectral phase can change greatly.)

MODEL RESPONSE FUNCTION CALCULATIONS OF THE POLARIZATION EMISSION TIME

The experimentally determined signal emission times are fit to various models of the material response function. Both the electronic (hyper)polarizability and nuclear response are included in models of the material response, giving rise to the anisotropic signal field of CS_2. A delta-function is used to represent the instantaneous electronic response of the liquid. Functions to describe the nuclear response are based on those used to

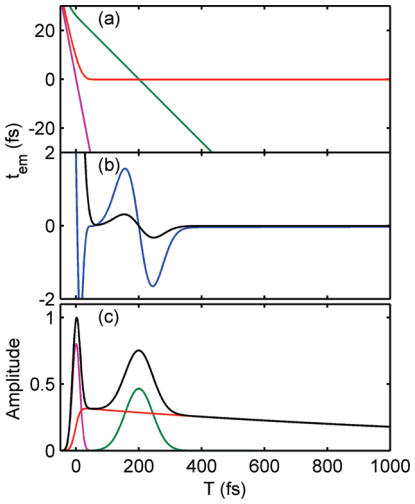

Figure 3. (a) Calculated signal emission times for model material response functions showing the role of a delta function (purple), used to model the electronic response, a Gaussian function centered at T = 200 fs (green), similar to the function used to model the librational nuclear response, and an exponential decay (red), which describes the rotational diffusion at long delays. (b) Emission times calculated from the sum of these terms (black) compared to the (amplitude weighted) sum of the emission times for each term (blue) show that the emission time is not additive. (c) Pump pulse convoluted with each term to show the relative amplitudes of the delta function (purple), Gaussian (green), exponential decay (red), and their sum (black).

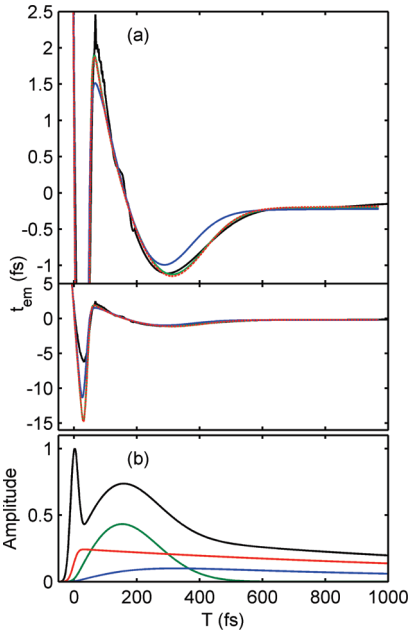

Figure 4. (a) Smoothed experimental signal emission times (black) shown on two scales with emission times modeled using eq 4 for the rotational diffusion (green), rotational diffusion with a rise matching the decay of librations (blue), and eq 14 for the rotational diffusion (red dashed). In all cases librations and II motions were modeled with eqs 5 and 6. Note that the red and green curves are nearly coincident. (b) Pump pulse convoluted with the response function to show the relative contribution of each component. The full model (black) is the sum of the electronic hyperpolarizability, the rotational diffusion term (red), the librational term (green), and the term describing interaction induced motion (blue).

describe the results of OKE measurements and contain terms for rotational diffusion, interaction-induced motion and librational motion as described in the Background, i.e., eqs 4−6. A Nelder−Mead simplex algorithm is used to minimize the square differences between the calculated signal emission times and the smoothed experimental values.[63] Convergence of the simplex algorithm is confirmed by checking different initial conditions and by varying each parameter of the response function individually after a minimum is found. Fitted curves are only calculated for T > 45 fs to avoid delays when the assumption that the probe pulse arrives in the sample after the pump pulses might be expected to break down.

Each term in the material response function for CS_2 contributes a specific behavior to the emission times calculated from the full response function. A purely electronic response function causes the TG signal to follow the convolution of the pump and probe pulses and the calculated t_{em} decays linearly, as shown in Figure 3a. The electronic response of the liquid is thus responsible for the monotonic decay of the measured signal emission times at negative and short T shown in Figure 2c. Additional terms are needed to describe the nuclear response, which causes the two recurrences in the measured t_{em} at longer delays. Examples of these terms are shown in Figure 3a. A model response function consisting solely of an exponential decay, describing rotational diffusion at large T, causes a quick decay at small T, followed by a constant, negative t_{em} for T > 50 fs. The value of t_{em} at large T depends only on the exponential decay time constant and pulse duration. A Gaussian response function, similar to the function used to describe librations, gives a linearly decaying t_{em}. The slope depends on the width of the Gaussian (100 fs) and the calculated t_{em} = 0 at the maximum of the Gaussian (T = 200 fs). Combinations of these terms are dominated by the largest amplitude term for any particular delay. As shown in Figure 3b, the emission times calculated from the sum of the delta function, Gaussian, and exponential decay are not the same as the sum of the emission times for each term. Comparison with the amplitude of each model term (Figure 2c) demonstrates that the first recurrence occurs when the nuclear response amplitude is larger than the electronic response, the second decrease in the emission time is due to the librational motion and the second recurrence occurs as the librational term decreases and the rotational diffusion term dominates the signal.

As usually formulated, the full nuclear response functions have somewhat arbitrary mathematical forms to describe the rise of one or more of the terms. The exponential rise of the rotational diffusion term in eq 4 is also used in similar models for the II response. The Bucaro−Litovitz model of the II motion and the antisymmetrized Gaussian model of the librational motion do not contain arbitrary rise terms. Calculating the t_{em} with models for the nuclear response containing these exponential rise terms replicates the general trends in the signal emission times, as seen in Figure 4a, but leads to unphysical parameters for the nuclear response function. In particular, τ_{rise} from eq 4 approaches zero, implying that the rotational diffusion does not rise exponentially but has nonzero amplitude at T = 0. Attempts to model the PET with a nonzero exponential rise, or with a Gaussian rise term matching the decay of the librational motions, fit the experimental t_{em} poorly. (See Figure 4a here and the Supporting Information in ref 62.) Furthermore, the separation between the rise of the rotational diffusion and librational decay shows that the

Table 1. Parameters Obtained for the Best Fit to the Smoothed Experimental Data[a]

parameter		value
Libration		
	a_L	1.5
	ω_0	10 cm^{-1}
	$\Delta\omega$	48 cm^{-1}
II		
	a_{II}	0.013
	b	0.05
	ω_{II}	17 cm^{-1}
Orientational/Rotational Diffusion		
	a_{RD}	0.15
	c	0.0009
	τ_{RD}	1700 fs

[a] The librational term is given by an antisymmetrized Gaussian (eq 5, see Supporting Information for analytical Fourier transform), the Bucaro−Litovitz function (eq 6) was used for the II term, and the exact dipole−dipole correlation function (eq 14) was used for the orientational/rotational diffusion term.

librations do not act as a (short time) coherent motion that drives rotational diffusion.

The failure of this analysis motivates the need for a new form for the rotational diffusion term of the nuclear response. Several candidates for the material response function captured the signal emission times less successfully and are described in the Supporting Information.[62] We find that the signal emission times are well-fit by a response function containing the usual librational response term (eq 5), the Bucaro−Litovitz model for the intermediate motions (eq 6) and a rotational diffusion term that is associated with the dipole−dipole orientational time-correlation function. The latter arises from a Langevin equation treatment of two dipoles in a viscous fluid with Gaussian white noise and is given by[64]

$$R_{RD}^{(3)}(t) = a_{RD} \exp\{-[t - c + ce^{-t/c}]/\tau_{RD}\} \qquad (14)$$

where τ_{RD} is the rotational diffusion time constant, a_{RD} and c are constants with $c = I/\zeta$, where I is the moment of inertia and ζ is the friction coefficient. At short times this response is Gaussian in form, and at longer times it follows the usual exponential decay. This function does not satisfy the usual condition that the intermolecular nuclear response function be zero at $T = 0$. The mechanical argument for this requirement is that there is an inertial delay in the nuclear response as the molecules respond to the torque induced by the pump fields.[13] However, we believe that the nonzero population of molecules probed in the TG experiment at this delay reflects the fact that a set of molecules are "selected" by the pump pulses from the population of molecules already aligned with the pump fields. Therefore, the rise of this response is determined by the width of the pump pulses. As shown in Figure 4a, the experimental emission times are well-described by those calculated from the best set of parameters for this model ($R^2 = 0.999$). The parameters are given in Table 1. (Note that the best fit parameters were obtained by holding the parameter for the rotational diffusion time constant fixed at 1.7 ps, which is the well documented value of the exponential decay of CS_2 at ~298 K.) Thus, we believe this is a well motivated and improved solution for the nuclear response function.

The general characteristics of the new composite nuclear response function agree well with previous results. For comparison with OKE measurements, the time-profile of the full material response function and each component convoluted with the pump pulses is shown in Figure 4b. As is generally found,[31] the librational and rotational diffusion terms (eqs 5 and 14, respectively) are responsible for the majority of the nuclear response, while the intermediate time-scale motions, represented by the Bucaro−Litovitz line shape (eq 6), are a relatively minor component. However, the II term is necessary for a good-quality fit of the signal emission times even with the new model for the rotational diffusion term. Table 1 lists the parameters found for the new model of the material response function. The parameters agree well with those found previously by OKE experiments[31] for librations[30] and by scattering measurements for II motions.[38] The exception is b, the parameter controlling the rise of the Bucaro−Litovitz term (see eq 6), which is 0.05, rather than the theoretical value of 12/7 for molecular liquids.[38] The same value for this parameter was found for the best fit parameters for the material response function using eq 4 to describe the rotational diffusion. The difference between the theoretical value and our experimentally determined value can be attributed to the anisotropy of the CS_2 molecule and the breakdown of the assumption that only 2-body interactions occur in liquids (i.e., 3-body, etc., interactions are neglected in the Bucaro−Litovitz form). In addition, it may reflect the presence of cross-terms between the canonical types of motion described.

DISCUSSION AND CONCLUSIONS

The selectivity of the fitted models to the measured PET signals implies that the emission times provide an additional constraint for models of the material response function. Models of the librational and II motions have been frustrated by the lack of distinct structure in the OKE spectral densities.[31] Unlike the OKE spectral densities, the PET measurement and analysis presented here is most sensitive to changes in the response function at short delays. At long delays, the emission times are relatively insensitive to the material response function; for example, an increase of 1 ps in the rotational diffusion time constant results in less than a 1 fs change in the value of t_{em} at large T. The emission time measurement thus complements the OKE or transient-grating, etc. measurements of the intermolecular fluctuations of CS_2 providing additional information to aid in the development of models for the nuclear component of the material response function.

The change in the nuclear response function has implications for the interpretation of the molecular motions involved in the nuclear response. The exponential rise factor in the rotational diffusion term of the nuclear response given in eq 4 reflects the inertial delay in the response of the liquid molecules to the perturbing electric fields. The dipole−dipole correlation function reflects the distinction between motions driven by the pump fields (librations and interaction-induced motions) and realignment by rotational diffusion of those molecules selected by the pump field. Further work with the corrected form of the rotational diffusion response motivated by these FR-TG-PET measurements will make more accurate models for the librational and II terms of the nuclear response accessible. The dipole−dipole correlation function form of the rotational diffusion alters the (T-dependent) amplitude of the remaining librational and II motions. Our work also provides insight into the appropriate

physical models for these motions. The breakdowns seen in the Bucaro−Litovitz model for II motions show that future models must consider higher order interactions between molecules in liquids in addition to pairwise interactions.

The need for corrections to unphysical and arbitrary terms in the nuclear response functions describing the structural relaxation modes of pure liquids has also been addressed by Turton and Wynne.[32] Their work developed corrections to the functional forms used to describe α (rotational diffusion) and β (intermediate time scale) relaxations in water and a peptide model molecule. While signal emission time measurements are not especially sensitive to the longer-time decays important in distinguishing the α and β relaxations and the corrections they propose, the FR-PET approach could be useful in confirming correct forms for the rise of the α and β relaxations.

Finally, in past and recent work from our group[45,46,50] we have been motivated to devise relatively simple experiments that would give more clarity and deeper insights into the limits of information content that can be obtained. In particular, in revisiting linear spectroscopy of densely absorbing solutions we were able to obtain information about the response functions of HOD (in D_2O) that had only been thought possible to ascertain via third-order nonlinear measurements.[46] The present paper shows that one can directly measure (and model) the nonlinear polarization, rather than its time integral. We have demonstrated the greater insight this provides on appropriate physical models for liquid dynamics. This method and the associated insights should be extended to create more illuminating probes of chemical reaction dynamics in solution. While CS_2 is a convenient and well studied molecular liquid due to its large OKE signal, with sufficient pulse energies, PET measurements can be extended to other molecular liquids, their mixtures, and more complex solutions. Measurements from our group have determined emission times for solutions[11] and for solvent molecules involved in solvation of a reacting solute.[7] As demonstrated by this study, PET measurements are most sensitive to a liquid's material response function at relatively short delays and could be used to distinguish differences in the librational motion, and thus local structure, in a series of liquids or mixtures. Multiexponential decays are often seen in mixtures of liquids,[31] these could be resolved in some cases by performing PET measurements with relatively long pulses. Longer pulse durations than those used in this study give large, easily measurable $|t_{em}|$at large T.

■ ASSOCIATED CONTENT

Supporting Information. Discussion of the method used to calculate the signal emission times. A list and descriptions of the candidate nuclear response functions used to fit the experimental signal emission times, including response functions not discussed in the main text. Discussion of details of the results of curve fitting and fitting conditions. This material is available free of charge via the Internet at http://pubs.acs.org.

■ AUTHOR INFORMATION

Corresponding Author

*E-mail: nfschere@uchicago.edu.

Present Addresses

[†]Department of Chemistry, The University of North Carolina at Chapel Hill, Chapel Hill, NC 27599.

■ ACKNOWLEDGMENT

This work was supported by the National Science Foundation (CHE 0317009). N.F.S. acknowledges the John S. Guggenheim Foundation for a Fellowship. M.A.H. was supported by the Department of Defense (DoD) through the National Defense Science & Engineering Graduate Fellowship (NDSEG) Program. We thank Richard Stratt and Greg Engel for helpful conversations. We also thank Shaul Mukamel for 20 years of personal and published stimulation. This paper is a testament to the fact that we listened when he admonished us to "look ...".

■ REFERENCES

(1) Park, S.; Flanders, B.; Shang, X.; Westervelt, R. A.; Kim, J.; Scherer, N. F. *J. Chem. Phys.* **2003**, *118*, 3917–3920.
(2) Park, S.; Kim, J.; Scherer, N. F. *Ultrafast Phenomena XIV*; Springer-Verlag: Berlin, 2005; Vol. 79.
(3) Moran, A. M.; Park, S.; Scherer, N. F. *Chem. Phys.* **2007**, *341*, 344–356.
(4) Park, S.; Kim, J.; Moran, A. M.; Scherer, N. F. *Phys. Chem. Chem. Phys.* **2011**, *13*, 214–223.
(5) Underwood, D. F.; Blank, D. A. *J. Phys. Chem. A* **2003**, *107*, 956–961.
(6) Underwood, D. F.; Blank, D. A. *J. Phys. Chem. A* **2003**, *109*, 3295–3306.
(7) Moran, A. M.; Nome, R. A.; Scherer, N. F. *J. Chem. Phys.* **2007**, *127*, 184505.
(8) Moran, A. M.; Nome, R. A.; Scherer, N. F. *J. Phys. Chem. A* **2006**, *110*, 10925–10928.
(9) Schmidtke, S. J.; Underwood, D. F.; Blank, D. A. *J. Phys. Chem. A* **2005**, *109*, 7033–7045.
(10) Ryu, S.; Stratt, R. M. *J. Phys. Chem. B* **2004**, *108*, 6782–6795.
(11) Moran, A. M.; Nome, R. A.; Scherer, N. F. *J. Chem. Phys.* **2006**, *125*, 031101.
(12) Mukamel, S. *Principles of Nonlinear Optical Spectroscopy*; Oxford University Press: New York, 1995.
(13) Kalpouzos, C.; Lotshaw, W. T.; McMorrow, D.; Kenney-Wallace, G. A. *J. Phys. Chem.* **1987**, *91*, 2028–2030.
(14) Ruhman, S.; Joly, A. G.; Nelson, K. *J. Chem. Phys.* **1987**, *86*, 6563–6565.
(15) Ruhman, S.; Kohler, B.; Joly, A. G.; Nelson, K. *Chem. Phys. Lett.* **1987**, *141*, 16–24.
(16) McMorrow, D.; Lotshaw, W. T. *Chem. Phys. Lett.* **1991**, *178*, 69–74.
(17) McMorrow, D.; Lotshaw, W. T. *J. Phys. Chem.* **1991**, *95*, 10395–10406.
(18) Kohler, B.; Nelson, K. *J. Phys. Chem.* **1992**, *96*, 6532–6538.
(19) Chang, Y. J.; Castner, E. W., Jr. *J. Chem. Phys.* **1993**, *99*, 7289–7299.
(20) Palese, S.; Schilling, L.; Miller, R. J. D.; Staver, P. R.; Lotshaw, W. T. *J. Phys. Chem.* **1994**, *98*, 6308–6316.
(21) Vohringer, P.; Scherer, N. F. *J. Phys. Chem.* **1995**, *99*, 2684–2695.
(22) Feldstein, M. J.; Vohringer, P.; Scherer, N. F. *J. Opt. Soc. Am. B* **1995**, *12*, 1500–1510.
(23) Lotshaw, W. T.; McMorrow, D.; Thantu, N.; Melinger, J. S.; Kitchenham, R. *J. Raman Spectrosc.* **1995**, *26*, 571–583.
(24) Chang, Y. J.; Castner, E. W., Jr. *J. Phys. Chem.* **1996**, *100*, 3330–3343.
(25) Quitevis, E. L.; Neelakandan, M. *J. Phys. Chem.* **1996**, *100*, 10005–10014.
(26) Palese, S.; Mukamel, S.; Miller, R. J. D.; Lotshaw, W. T. *J. Phys. Chem.* **1996**, *100*, 10380–10388.
(27) Neelakandan, M.; Pant, D.; Quitevis, E. L. *J. Phys. Chem. A* **1997**, *101*, 2936–2945.
(28) Scodinu, A.; Fourkas, J. T. *J. Phys. Chem. B* **2002**, *107*, 44–51.

(29) Rajian, J. R.; Hyun, B.-R.; Quitevis, E. L. *J. Phys. Chem. A* **2004**, *108*, 10107–10115.
(30) Heisler, I. A.; Corriea, R. R. B.; Buckup, T.; Cunha, S. L. S.; da Silveira, N. P. *J. Chem. Phys.* **2005**, *123*, 054509.
(31) Zhong, Q.; Fourkas, J. T. *J. Phys. Chem. B* **2008**, *112*, 15529–15539.
(32) Turton, D. A.; Wynne, K. *J. Chem. Phys.* **2008**, *128*, 154516.
(33) Xiao, D.; Hines, L. G.; Bartsch, R. A.; Quitevis, E. L. *J. Phys. Chem. B* **2009**, *113*, 4544–4548.
(34) Geiger, L. C.; Ladanyi, B. M. *J. Chem. Phys.* **1987**, *87*, 191–202.
(35) Geiger, L. C.; Ladanyi, B. M. *Chem. Phys. Lett.* **1989**, *159*, 413–420.
(36) Murry, R. L.; Fourkas, J. T.; Keyes, T. *J. Chem. Phys.* **1998**, *109*, 2814–2825.
(37) Murry, R. L.; Fourkas, J. T.; Li, W.-X.; Keyes, T. *Phys. Rev. Lett.* **1999**, *83*, 3550–3553.
(38) Bucaro, J. A.; Litovitz, T. A. *J. Chem. Phys.* **1971**, *54*, 3846–3853.
(39) Trebino, R. *Frequency Resolved Optical Gating: The Measurement of Ultrashort Laser Pulses*; Kluwer: Boston, Dordrecht, London, 2000.
(40) Lepetit, L.; Chériaux, G.; Joffre, M. *J. Opt. Soc. Am. B* **1995**, *12*, 2467–2474.
(41) Tokunaga, E.; Terasaki, A.; Kobayashi, T. *J. Opt. Soc. Am. B* **1995**, *12*, 753–771.
(42) Gallagher, S. M.; Albrecht, A. W.; Hybl, J. D.; Landin, B. L.; Rajaram, B.; Jonas, D. M. *J. Opt. Soc. Am. B* **1998**, *15*, 2338–2345.
(43) Iaconis, C.; Walmsley, I. A. *Opt. Lett.* **1998**, *23*, 792–794.
(44) McGrane, S. D.; Scharff, R. J.; Barber, J. *J. Opt. Soc. Am. B* **2006**, *23*, 2217–2222.
(45) Gruetzmacher, J. A.; Scherer, N. F. *Opt. Lett.* **2003**, *28*, 573–575.
(46) Gruetzmacher, J. A.; Nome, R. A.; Moran, A. M.; Scherer, N. F. *J. Chem. Phys.* **2008**, *129*, 224502.
(47) de Boejj, W. P.; Pshenichnikov, M. S.; Wiersma, D. A. *Annu. Rev. Phys. Chem.* **1998**, *49*, 99–123.
(48) Lang, M. J.; Jordanides, X. J.; Song, X.; Fleming, G. R. *J. Chem. Phys.* **1999**, *110*, 5884–5892.
(49) Yang, T. S.; Vohringer, P.; Arnett, D. C.; Scherer, N. F. *J. Chem. Phys.* **1995**, *103*, 8346–8359.
(50) Book, L. D.; Scherer, N. F. *J. Chem. Phys.* **1999**, *111*, 792–795.
(51) Jonas, D. M. *Annu. Rev. Phys. Chem.* **2003**, *54*, 425–463.
(52) Brixner, T.; Stenger, J.; Vaswani, H. M.; Cho, M.; Blankenship, R. E.; Fleming, G. R. *Nature* **2005**, *434*, 625–628.
(53) Read, E. L.; Engel, G. S.; Calhoun, T. R.; Mancal, T.; Ahn, T. K.; Blankenship, R. E.; Fleming, G. R. *Proc. Nat. Acad. Sci. U. S. A.* **2007**, *104*, 14203–14208.
(54) Asplund, M. C.; Zanni, M. T.; Hochstrasser, R. M. *Proc. Nat. Acad. Sci. U. S. A.* **2000**, *97*, 8219–8224.
(55) Asbury, J. B.; Steinel, T.; Stromberg, C.; Corcelli, S. A.; Lawrence, C. P.; Skinner, J. L.; Fayer, M. D. *J. Phys. Chem. A* **2004**, *108*, 1107–1119.
(56) Ishikawa, H.; Kim, S.; Kwak, K.; Wakasugi, K.; Fayer, M. D. *Proc. Nat. Acad. Sci. U. S. A.* **2007**, *104*, 19309–19314.
(57) Kuo, C. H.; Hochstrasser, R. M. *Chem. Phys.* **2007**, *341*, 21–28.
(58) Liau., Y.-H.; Unterreiner, A. N.; Arnett, D. C.; Scherer, N. F. *Appl. Opt.* **1999**, *38*, 7386–7392.
(59) Khalil, M.; Golonzka, O.; Demirdoven, N.; Fecko, C. J.; Tokmakoff, A. *Chem. Phys. Lett.* **2000**, *321*, 231–237.
(60) Etchepare, J.; Grillon, G.; Arabat, J. *Appl. Phys. B: Lasers Opt.* **1989**, *49*, 425–429.
(61) Herzberg, G. *Molecular Spectra and Molecular Structure: II. Infrared and Raman Spectra of Polyatomic Molecules*; Litton Educational Publishing, Inc.: New York, 1945.
(62) Hershberger, M. A.; Moran, A. M.; Scherer, N. F. Supporting Information for this paper; http://dx.doi.org/10.1021/jp111796d.
(63) Nelder, J. A.; Mead, R. *Comput. J.* **1965**, *7*, 308–313.
(64) Zwanzig, R. *Nonequilibrium Statistical Mechanics*; Oxford University Press: London, 2001.